CERES Terra and Aqua Edition4 CRS Data Quality Summary

Version 1
Updated 5/3/2023

Investigation: **CERES**

Data Product: **Clouds and Radiative Swath (CRS)**

Data Set: **Terra (Instruments: CERES-FM1, MODIS)**
Aqua (Instruments: CERES-FM3, MODIS)

Data Set Version: **Edition4A** **Release Date: May 5, 2023**

Subsetting Tool Availability: https://ceres.larc.nasa.gov/data/

The purpose of this document is to inform users of the accuracy of this data product as determined by the CERES (Wielicki et al., 1996) Science Team. This document briefly summarizes key validation results, provides cautions where users might easily misinterpret the data, provides links to further information about the data product, algorithms, and accuracy, and gives information about planned data improvements.

This document is a high-level summary and represents the minimum necessary information for scientific users of this data product. It is strongly suggested that authors, researchers, and reviewers of research papers re-check this document (especially Cautions and Helpful Hints) for the latest status before publication of any scientific papers using this data product.

TABLE OF CONTENTS

Section Page

LIST OF FIGURES

Figure Page

LIST OF TABLES

Table Page

1.0 Nature of the Clouds and Radiative Swath (CRS) Product

The Clouds and Radiative Swath (CRS) product consists of top-of-atmosphere (TOA), within-atmosphere, and surface radiative fluxes from radiative transfer model calculations initialized using observed-based input data sources. CRS development is evolutionary—new versions are released as algorithm and input dataset improvements are implemented. The present document describes how Edition4A CRS fluxes are computed from input variables and what the uncertainty ranges of the computed fluxes are. A more complete description of CRS Edition 4A (Ed4A) is described in Scott et al. (2022).

1.1 Introduction

The CRS product (Figure 1-1) is designed for understanding radiant energy flows within the atmosphere and at the surface by computing radiative fluxes from the TOA to surface. The CRS computed fluxes are produced for shortwave (SW), longwave (LW), and window (WN; 8.0-12.0 μm), both upwelling and downwelling at TOA, 70 hPa, 200 hPa, 500 hPa, 850 hPa, and the surface (Figure 1). To permit the user to infer cloud radiative effect and direct aerosol radiative effect, fluxes are provided for all-sky (clouds+aerosol), clear (aerosol only), no-aerosol (clouds only), and pristine conditions (no clouds and aerosol). Like its parent Single Scanner Footprint (SSF) product, the CRS product corresponds to an instantaneous CERES footprint. The footprint has a nominal nadir resolution of 20 km for half power points but the size increases with the viewing angle (Figure 1-2).

The CRS data product includes CERES-observed TOA fluxes and some Moderate-Resolution Imaging Spectroradiometer (MODIS) cloud properties from the SSF product. Additional SSF footprint variables can be obtained from the SSF product and linked to footprints in CRS through the CERES footprint identification numbers (“Scan sample number” and “Packet number”), which consistently identify footprints in both products.

Users are also encouraged to visit the CERES ordering tool, which enables user-specified CRS parameters to be ordered, thereby reducing data volume (the full product size is 700 megabytes per day). An online version of the radiative transfer code used to produce the CRS product can be found here.

The CERES team plans to eventually release a gridded version of CRS, called CRS1deg. As CRS is an instantaneous product, it only provides data at CERES observation times. For full diurnal coverage, users are encouraged to use the SYN1deg product, which provides hourly 1°×1° surface fluxes. Users may benefit from the CERES Archival Data website to help determine the most suitable CERES data product to use.

When referring to a CERES dataset, please include the satellite name and/or the CERES instrument name, the dataset version, and the data product. Multiple files which are identical in all aspects of the filename except for the 6-digit configuration code (see Collection Guide - when available) differ little, if any, scientifically. Users may, therefore, analyze data from the same satellite/instrument (here Aqua/CERES/MODIS), data set version (here Edition4A), and data

product (here CRS) without regard to configuration code. This CRS dataset may be referred to as "CERES Terra or Aqua Edition4A CRS".

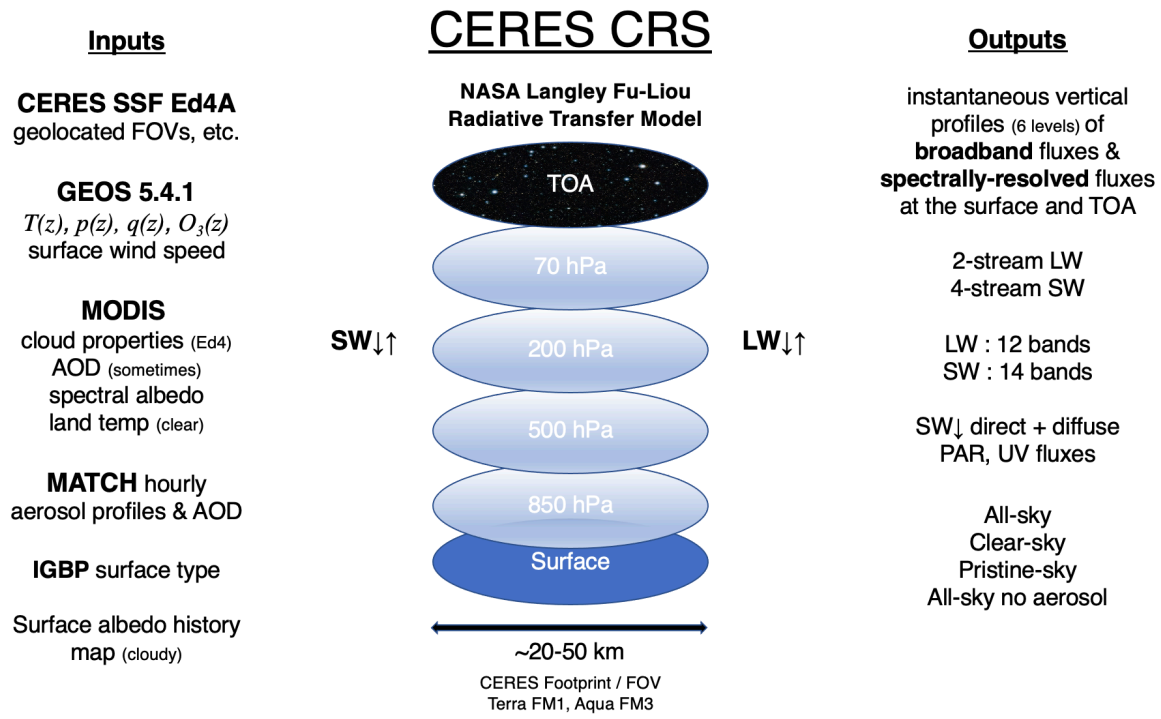

Figure 1-1. Illustration of the CERES CRS Ed4 flux computation algorithm (Scott et al. 2022).

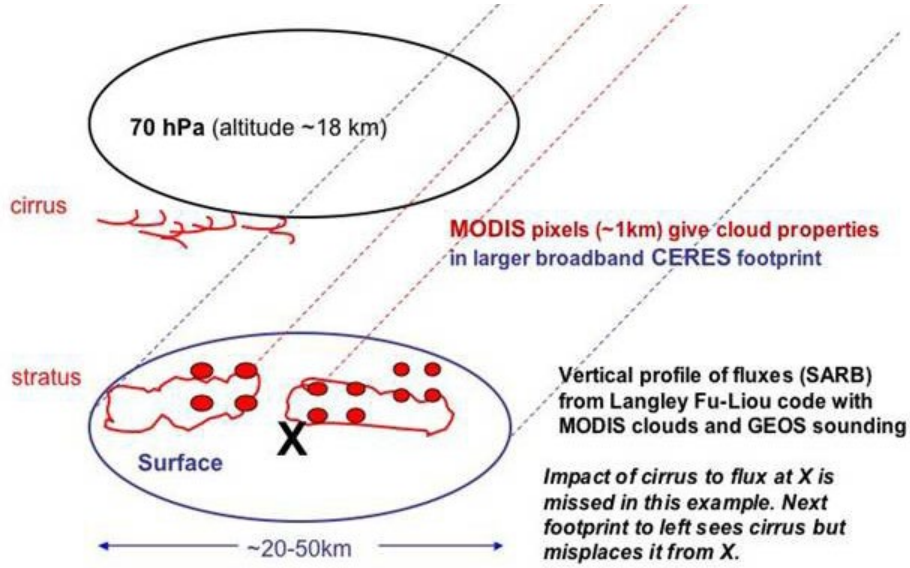

Figure 1-2. Typical viewing geometry showing small MODIS pixels within large CERES footprints. Output levels at TOA, 200 hPa, 500 hPa, and 850 hPa are not drawn in the figure.

1.2 Description of the Edition4 CRS Product

Originally developed by the CERES science team in the 2000s, CRS extends the standard L2 SSF data product by calculating radiative fluxes at the instantaneous footprint scale using the NASA Langley Fu–Liou (LFL) RTM. CRS data were previously released with CERES Edition 2B (Ed2B) data products, covering July 2002 to April 2006 that used MODIS collection 4 radiances (Rutan et al. 2009; Rose et al. 2013). The following version, Edition 2C, used MODIS collection 5 radiances, and the processing was initiated in May 2006. However, the CRS processing ceased shortly thereafter owing to high computational cost and a greater need to prioritize the development of CERES level 3 (L3) gridded data products used for climate model evaluation.

The resumed CRS product with Ed4 algorithm will cover 5 years from 2018 to 2022. The new algorithm uses improved and more recent versions of input datasets, expecting a better accuracy of computed fluxes, compared to the earlier CRS versions. However, a direct comparison between the earlier versions and Ed4 computed fluxes is not possible due to the no overlapping periods.

Input variables used for the Ed4 CRS flux algorithm are described in Scott et al. (2022). The CRS algorithm uses 6-hourly gridded fields of temperature, humidity, and ozone profiles contained in the Meteorological, Ozone, and Aerosol (MOA)-5.4.1 product, which was generated from the Global Modeling and Assimilation Office (GMAO) Goddard Earth Observing System (GEOS)-5.4.1 system. MOA-5.4.1 is not publically available but GEOS-5.4.1 is available on request to the GMAO team. The cloud properties are based on the CERES-MODIS Ed4 cloud algorithm (Minnis et al. 2021) using MODIS Collection 6 narrowband radiances. Aerosol optical properties are from MODIS Collection 6 MOD04/MYD04 (Remer et al. 2005; Ignatov et al. 2005; Levy et al. 2013) retrieved for clear-sky scenes. Also, the hourly Atmospheric Transport and Chemistry (MATCH) (Collins et al. 2001; Fillmore et al. 2022) product is used for filling aerosol properties for cloudy scenes. Ocean surface albedo is from the empirical model (Jin et al. 2004). Land surface albedo is from the Collection 6 MODIS bidirectional reflectance direction function (BRDF) (MCD43C1) product (Strahler et al. 1999). Snow/ice surface albedo is described by the surface history albedo (SAH) map, which was derived from clear-sky CERES measurements (Rutan et al. 2009, Radkevich et al. 2013). Skin temperatures are retrieved from clear-sky MODIS 11-μm channel observations by the CERES-MODIS Ed4 cloud algorithm (Minnis et al. 2021). If the MODIS-retrieved skin temperature is not available for overcast conditions, MOA skin temperature is used. NASA Langley Fu-Liou model (Fu and Liou 1993; Kratz and Rose 1999; Kato et al. 1999, 2005) is used for radiative simulations.

The CRS main output parameters are computed radiative fluxes at TOA, 70 hPa, 200 hPa, 500 hPa, 850 hPa, and surface. Note that one pressure level (i.e., 850 hPa) is added for the Ed4A version. Unlike the previous versions of CRS product, Ed4A CRS does not provide tuned computed fluxes. This is because the uncertainty in observed TOA instantaneous fluxes is large (~5%) so the observed fluxes do not provide a tight constraint. In addition, even if the tuning process was shown to improve TOA flux simulations, it does not necessarily improve surface flux simulations because instantaneous TOA and surface fluxes are often decoupled (Rose et al. 2013; Scott et al. 2022). Therefore, for the Ed4 CRS product, we only provide untuned computed fluxes. Eliminating the tuning process drastically reduces the amount of time required for the CRS Ed4 processing.

2.0 Cautions and Helpful Hints

- As mentioned earlier, the CRS product only includes a subset of SSF variables (e.g., CERES-derived TOA fluxes and some of the MODIS cloud parameters). Users who require additional SSF variables can do so by linking CRS and SSF footprints using the CERES footprint identification numbers (called “Scan sample number” and “Packet number”). Note that most of the time SSF and CRS contain the same number of CERES footprints with consistent ordering. The footprint identification numbers can be used to verify them.
- The CRS data sets contain only every other CERES footprint when the viewing zenith is less than 63°. All footprints with a viewing zenith greater than or equal to 63° are included in the CRS. When "CERES viewing zenith at surface," is less than 63° and "Packet number," is even, then only footprints with an even value in "Scan sample number," are placed on the CRS. When "CERES viewing zenith at surface" is less than 63° and "Packet number" is odd, then only footprints with an odd value in "Scan sample number" are placed on the CRS. The CERES footprints are sufficiently overlapped in the scanning direction that this use of every other footprint does not leave gaps in the data spatial coverage or significantly increase errors in gridded data products or instantaneous comparisons to surface data such as BSRN.
- Before using CRS parameter values, users should check for CERES default values. CERES default values, or fill values, are very large values which vary by data type. A CERES default value is used when the parameter value is unavailable or considered suspect.
- When the 850 hPa level is below the surface, the values are CERES default.
- The geographic location of a CERES flux estimate is at the surface geodetic latitude and longitude of the CERES footprint centroid.
- A footprint is recorded in the hourly CRS file that contains its observation time. However, CRS footprints within the file are ordered on alongtrack angle (not included) and not on time.
- The Total Solar Irradiance (TSI) daily fluxes used in calculating the “TOA Incoming Solar Radiation – SSF” parameter during August 2019 and May through November 2020. were found to be scaled incorrectly resulting in a daily flux that was biased ~+0.8 Wm^{-2}. The incorrect daily TSI fluxes (based on TSIS-1 TIM Version 3) were correctly scaled to SORCE Version 15 reference for latter processing. The impact on the Incoming Solar Radiation is reduced by the factor of pi from the TSI.

3.0 Accuracy and Validation

The CRS product includes CERES Ed4A observed TOA fluxes for the validation of the computed fluxes at the TOA level. At the surface, the computed fluxes can be validated with ground-based measurements. Thorough validation of CRS Ed4 fluxes was performed by Scott et al. (2022), and here we provide the summary of the work.

Figure 3-1 shows the biases of the CRS-computed reflected SW (RSW) at TOA with respect to CERES Ed4A observations. The daytime global mean positive biases are around 2%–5% (6–11 W m^{-2}) (Figure 3-1c). Cloud reflection errors, which are most pronounced for high-level ice clouds, are the primary driver of this bias. The biases are related to ice particle size biases (Ham et al. 2022) or the ice crystal habit model (Loeb et al. 2018) used for computations. Partly cloudy pixels also might have impacted the SW biases (Ham et al. 2021).

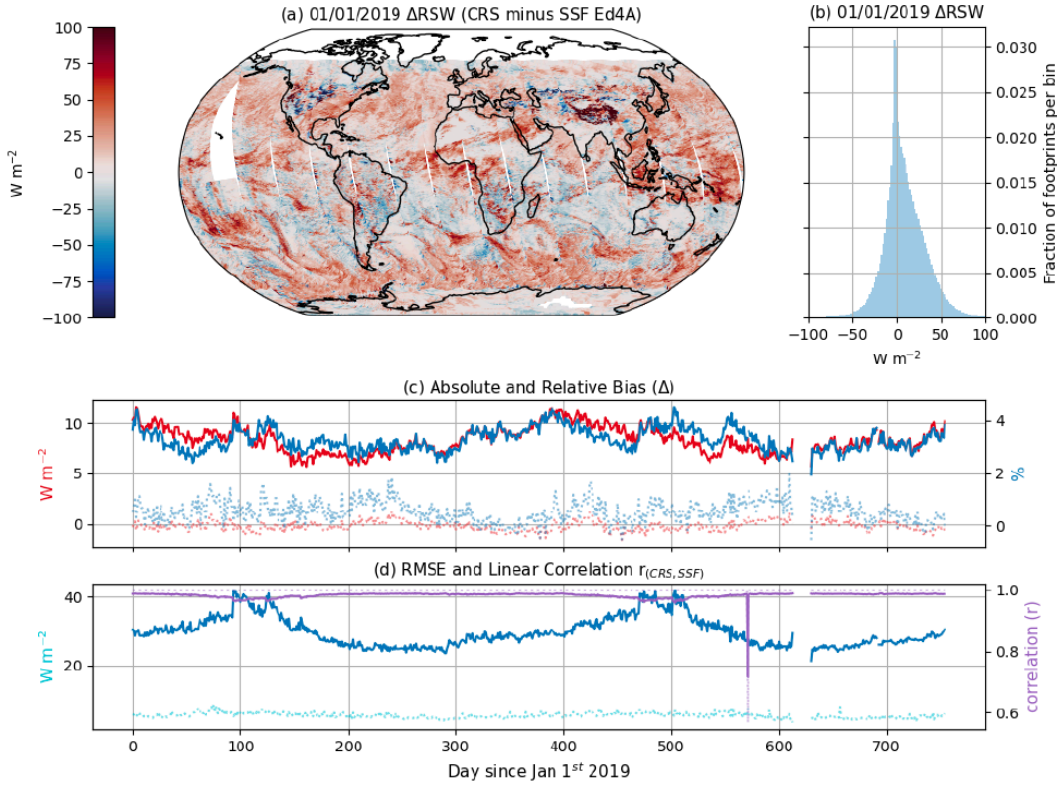

Figure 3-1: CERES Aqua FM3 CRS daytime SW TOA flux validation statistics relative to SSF Ed4A observations. Panel (a) shows a map of the instantaneous CRS computed reflected SW radiation (RSW) minus the SSF Ed4A observed RSW on January 1, 2019, while panel (b) shows a histogram of the instantaneous flux bias ΔRSW. The subsequent panels present a time series of daily validation statistics for the period January 1, 2019 - December 31, 2020, including (c) the planetary mean absolute bias (red) and relative bias (blue), and (d) the RMS (cyan) and Pearson linear correlation coefficient A (purple). All means are computed by weighting each CERES footprint by cos ϕ, where ϕ is latitude. All-sky planetary means are

depicted by solid curves. Results for clear-sky footprints (cloud fraction = 0%) only are depicted by dashed curves.

Comparison between computed CRS computed LW outgoing longwave radiation (OLR) with CERES Ed4A observations in Figure 3-2 and Figure 3-3 shows that the computed LW fluxes are negatively biased, but the biases remain within 1% (2–3 W m^{-2}). The biased LW upward TOA fluxes are largely associated with clear-sky footprints, which suggests that the GEOS-5.4.1 atmosphere may be too cold and/or moist, or skin temperature biases. The overall negative LW TOA biases are partially compensated by positive biases associated with high-level ice clouds (Figure 3-2a and Figure 3-3a). A slight discontinuity in clear-sky OLR bias and RMSD at nighttime (Figure 3-3) is related to microwave humidity sounder instrument loss and subsequent lack of data assimilation in GEOS 5.4.1 in November 2019 (around 330 days since January 1st, 2019).

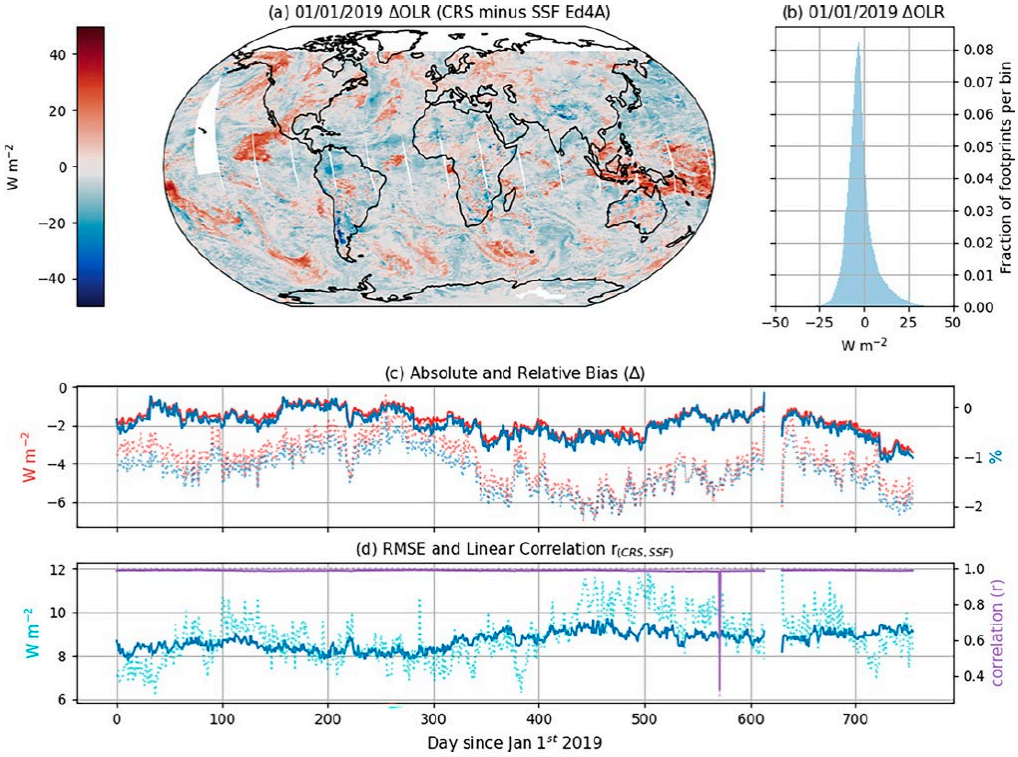

Figure 3-2. Same as Figure 3-1 but for daytime outgoing longwave radiation (OLR) (W m^{-2}).

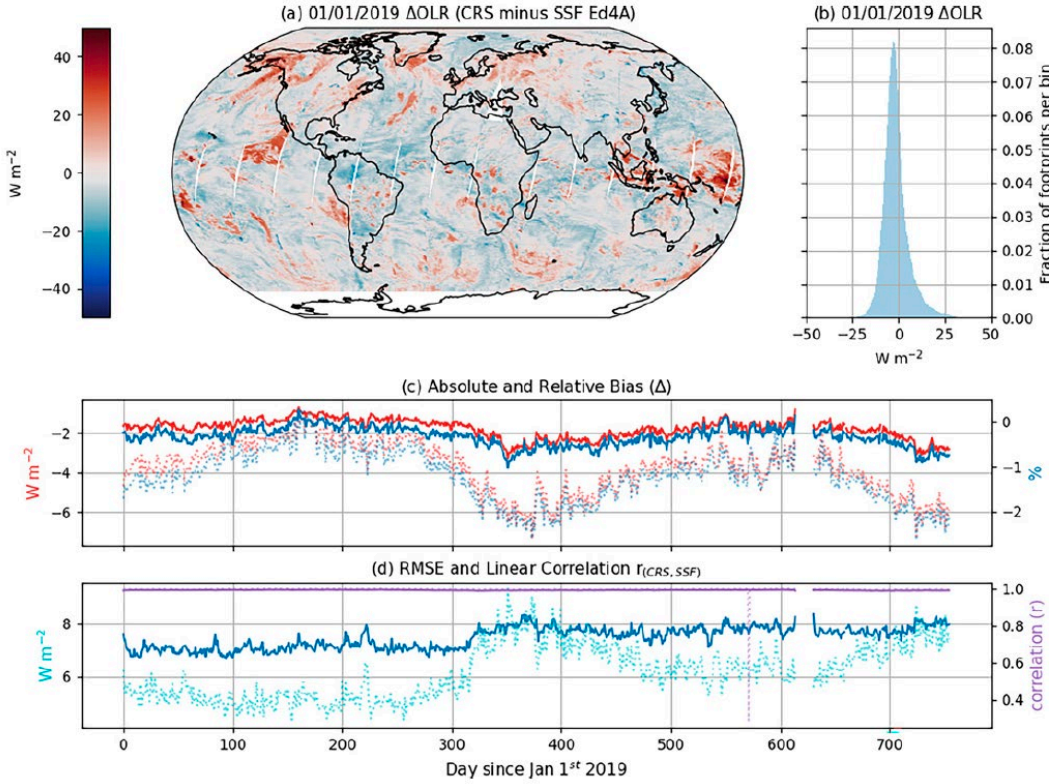

Figure 3-3. Same as Figure 3-1 but for nighttime OLR.

We now shift to a comparison of Aqua Ed4 CRS with surface ground measurements (ground sites are shown in Fig. 2 of Scott et al. 2022). Besides the CRS computed fluxes, we also consider two additional parameterized surface flux variables (i.e., "SSF Model B" and "FLASHFlux Model B") in the validation. "SSF Model B" fluxes are available in the CERES SSF Ed4 product and these are produced to supplement the CERES TOA flux satellite observations (Gupta 1989; Gupta et al. 1992; Gupta 2001; 2010). The SSF Model B algorithm estimates the surface broadband SW downward flux by accounting for the transmission of the incoming solar beam through clear and cloudy atmospheric layers (Gupta 2001). The SSF Model B algorithm also estimates the surface broadband LW downward flux in terms of an effective atmospheric emission temperature, cloud amount and base height, and sub-cloud column-integrated water vapor (Gupta 1989; Gupta et al. 1992). The parameterized fluxes by the FLASHFlux working group ("FLASHFlux Model B") also use a similar approach to "SSF Model B" but expedites the SSF processing to provide fluxes in near-real time (Kratz et al. 2014) using GMAO GEOS Forward Processing for Instrument Teams (FP-IT) meterological assimilation data. These near-real-time fluxes are useful for clean energy, infrastructure energy use, and agricultural applications.

Figure 3-4 compares the performance of the all-sky broadband SW downward surface flux computations from CRS, SSF Model B, and FLASHFlux Model B at the ground sites for two-year period (January 2019 to December 2020). The CRS SW surface downward fluxes are negatively biased to observations, whereas SSF Model B shows a smaller negative mean bias and FLASHFlux

Model B shows a relatively large positive mean bias. However, a smaller root-mean-square difference (RMSD) value is noted in the CRS flux, compared to SSF Model B or FLASHFlux Model B. The CRS SW surface downward fluxes also correlate more strongly with the measured fluxes than their parameterized counterparts (Model B or FLASHFlux) do. These statistics are further decomposed by surface type and cloud conditions in Table 3-1. CRS produces an improved SW downward RMSD and linear correlation coefficient (r) over every surface type, regardless of cloud conditions, compared to two other parameterized flux SW variables.

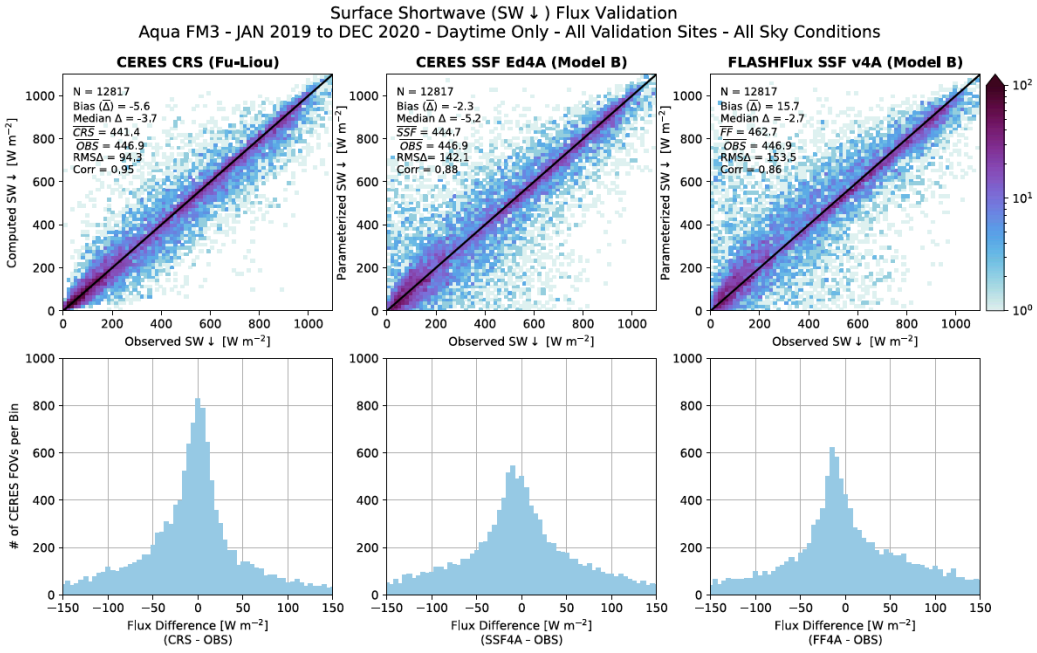

Figure 3-4: Comparison of the CERES Aqua FM3 CRS daytime all-sky surface SW downward fluxes to measurements from a globally distributed network of surface observation sites during 2019/20. Results are also presented for (center) the SW Model B surface flux parameterization algorithm from the CERES SSF Edition 4A and (right) FLASHFlux Model B version 4A. (top) Joint histograms indicating the number of values within each bin. (bottom) Histograms of the instantaneous flux difference. N denotes the total number of samples.

Table 3-1. Breakdown of the computed SW downward flux validation statistics according to surface type and cloud conditions. In cells with multiple entries, the values correspond to CRS, SSF Model B, and FLASHFlux Model B, respectively. The dataset with the best statistic is highlighted in boldface font. The mean flux, mean and median flux bias, and RMS flux difference are expressed in units of W m^{-2}. The correlation (r) is the Pearson linear correlation coefficient. The global category combines data from all sites. Overcast-sky comparisons include footprints with a cloud fraction < 95% in all products. Clear-sky comparisons include footprints with a cloud fraction < 5% in all products.

	N	Mean flux	Bias ($\overline{\Delta}$)	Median Δ	RMSΔ	Correlation (*r*)
All-sky SW↓						
Global	12 817	441.4, 444.7, 462.7	−5.6, **−2.3**, 15.7	−3.7, −5.2, **−2.7**	**94.3**, 142.1, 153.5	**0.95**, 0.88, 0.86
Coastal	2443	464.8, 482.5, 478.5	**−5.9**, 11.9, 7.8	−8.5, **0.8**, −5.6	**99.0**, 124.7, 135.3	**0.93**, 0.90, 0.87
Desert	822	795.7, 803.4, 791.4	−11.5, **−3.8**, −15.8	−7.3, **−5.1**, −14.0	**75.9**, 86.1, 89.4	**0.93**, 0.91, 0.90
Island	604	644.3, 663.1, 669.9	**53.8**, 72.6, 79.4	**13.9**, 37.2, 43.9	**159.5**, 173.2, 185.9	**0.84**, 0.82, 0.79
Continental	4754	514.5, 524.5, 530.7	**−1.0**, 9.0, 15.2	**−1.1**, 5.2, 2.2	**103.8**, 115.7, 126.8	**0.93**, 0.91, 0.89
Polar	4194	246.1, 230.4, 282.2	**−18.0**, −33.7, 18.1	**−5.1**, −27.2, −8.4	**67.0**, 177.9, 191.3	**0.95**, 0.60, 0.57
Overcast-sky SW↓						
Global	5572	262.7, 274.1, 309.2	−9.0, **2.4**, 37.5	**−5.1**, 5.6, 27.1	**91.8**, 155.5, 174.3	**0.90**, 0.73, 0.69
Coastal	1197	294.8, 319.0, 321.6	**−3.9**, 20.3, 22.9	**−2.6**, 20.1, 19.6	**86.4**, 137.0, 154.4	**0.92**, 0.80, 0.74
Desert	74	510.3, 548.4, 532.0	−14.6, 23.5, **7.1**	**−4.2**, 27.6, 27.9	**128.0**, 159.5, 166.2	**0.87**, 0.81, 0.78
Island	216	454.7, 480.4, 496.7	**64.9**, 90.6, 106.9	**43.4**, 73.9, 82.9	**163.3**, 186.4, 214.2	**0.81**, 0.78, 0.71
Continental	1862	302.0, 322.3, 336.7	**−0.7**, 19.7, 34.1	**1.0**, 25.6, 35.8	**94.9**, 111.3, 138.1	**0.90**, 0.87, 0.81
Polar	2223	185.7, 180.4, 253.9	**−25.7**, −31.0, 42.5	**−12.5**, −29.1, 14.7	**80.1**, 189.5, 204.8	**0.90**, 0.35, 0.44
Clear-sky SW↓						
Global	2922	608.7, 601.8, 596.3	**−1.8**, −8.74 −14.3	**1.3**, −7.9, −14.7	**35.4**, 128.8, 145.3	**0.99**, 0.89, 0.86
Coastal	318	663.3, 670.2, 656.5	−4.4, **2.6**, −11.2	**−4.9**, −8.0, −24.0	**31.9**, 132.5, 143.6	**0.99**, 0.78, 0.74
Desert	570	839.8, 837.9, 822.8	**−9.8**, −11.7, −26.8	**−3.5**, −5.7, −15.8	**35.4**, 58.0, 65.7	**0.98**, 0.94, 0.93
Island	41	870.0, 872.2, 860.6	**1.6**, 3.8, −7.9	**−0.2**, 1.7, −4.6	**29.1**, 41.6, 45.5	**0.97**, 0.94, 0.94
Continental	1000	704.8, 699.0, 690.7	4.7, **−1.1**, −9.4	3.0, **−1.2**, −11.1	**39.9**, 61.8, 73.5	**0.98**, 0.95, 0.93
Polar	993	351.3, 335.5, 341.0	**−3.1**, −18.8, −13.4	**2.3**, −16.3, −17.7	**31.6**, 193.3, 218.0	**0.99**, 0.60, 0.49

Figure 3-5 and Figure 3-6 compare all-sky broadband LW downward surface flux biases of CRS, SSF Model B, and FLASHFlux Model B at the ground-based network sites during day and night, respectively. During the daytime, CRS shows the smallest mean bias and an RMSD, compared to SSF Model B and FLASHFlux Model B (Figure 3-5). At night, CRS shows a negative mean bias, while is comparable to the SSF Model B (Figure 3-6). However, RMSD values of CRS fluxes are smaller than those of SSF Model B or FLASHFlux Model B. Also higher correlation coefficients are noted from CRS fluxes, compared to the other two parameterized fluxes.

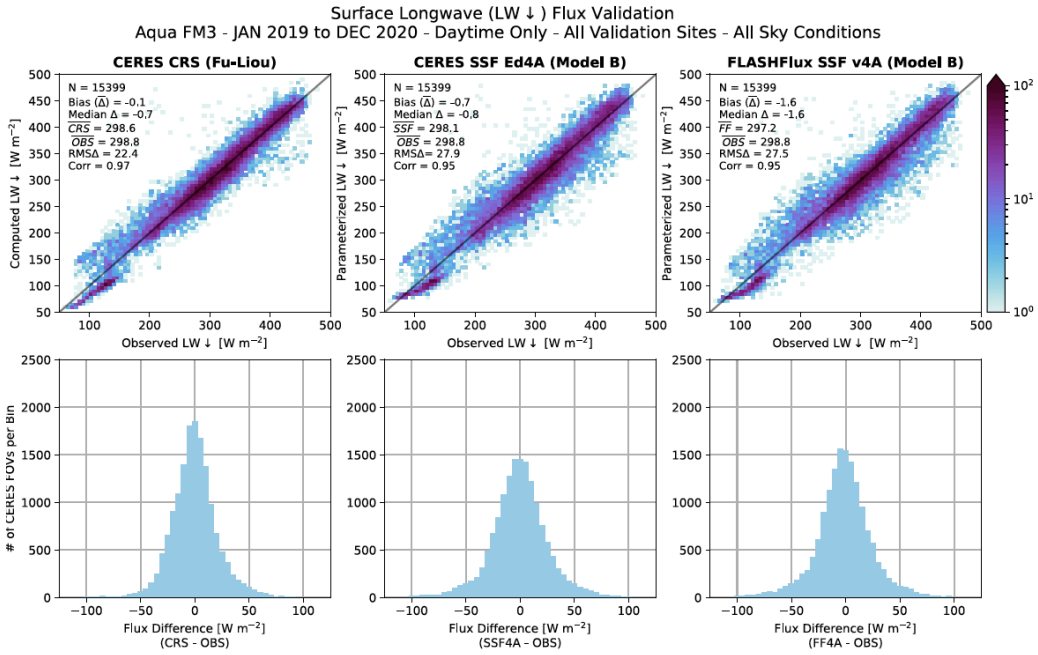

Figure 3-5: Same as Figure 3-4 but for daytime LW surface downward flux validation.

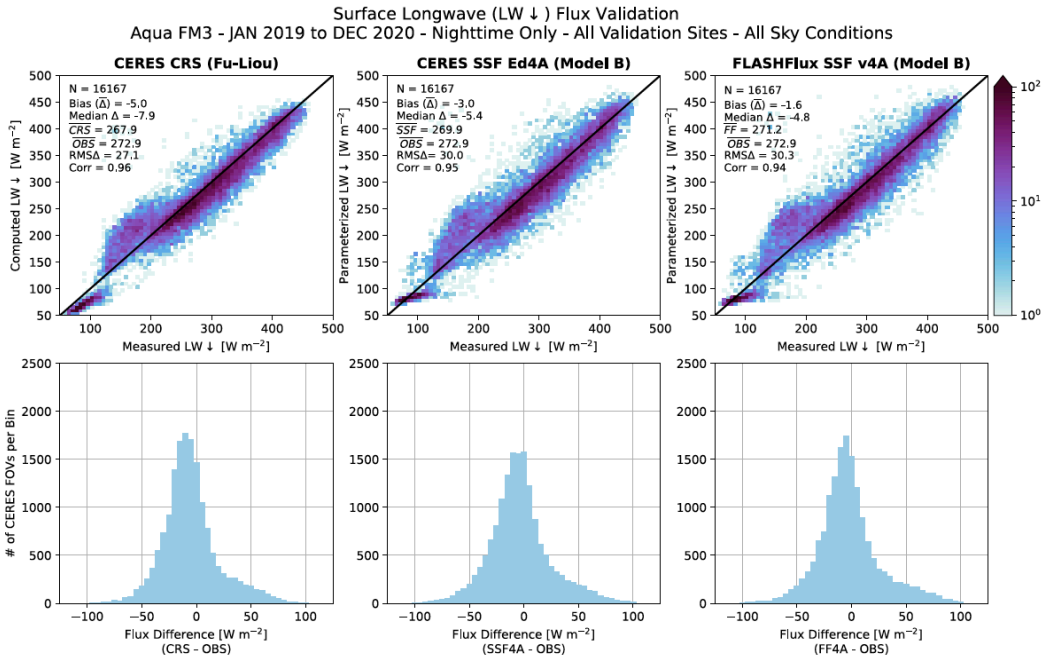

Figure 3-6: Same as Figure 3-4 but for nighttime LW surface downward surface validation.

In Table 3-2 and Table 3-3, better performance of the CRS LW fluxes is generally shown compared to SSF and FLASHFlux Model B, in terms of RMSD and correlation coefficient r, over every surface type, independent of cloud conditions. The only exception is for clear-sky polar fluxes at night (Table 3-3). Negative nighttime LW downward biases are likely in part linked to poor cloud optical thickness information, which is difficult to retrieve with only infrared channels and

translates to overestimates of cloud-base height (Minnis et al. 2020; Yost et al. 2020).

Table 3-2: Same as Table 3-1 but for daytime LW surface downward flux.

	N	Mean flux	Bias ($\overline{\Delta}$)	Median Δ	RMSΔ	Correlation (*r*)
All-sky LW↓						
Global	15 399	298.6, 298.1, 297.2	−**0.1**, −0.7, −1.6	−**0.7**, −0.8, −1.6	**22.4**, 27.9, 27.5	**0.97**, 0.95, 0.95
Coastal	2904	350.5, 346.9, 345.8	4.2, 0.6, −**0.5**	3.3, 1.8, **1.1**	**15.7**, 26.5, 26.1	**0.97**, 0.91, 0.91
Desert	932	335.3, 342.1, 341.0	−16.8, −**10.0**, −11.0	−14.7, −7.2, −**5.1**	**28.6**, 33.7, 31.1	**0.89**, 0.78, 0.82
Island	735	411.3, 414.1, 413.6	**2.2**, 5.0, 4.5	**2.3**, 4.6, 4.5	**14.9**, 18.6, 19.4	**0.84**, 0.82, 0.8
Continental	5251	330.5, 327.6, 325.3	3.3, **0.3**, −1.9	2.1, 1.4, −**0.6**	**22.8**, 27.5, 28.2	**0.93**, 0.9, 0.9
Polar	5577	220.6, 222.3, 223.7	−3.1, −1.5, −**1.1**	−6.7, −4.8, −**4.5**	**24.5**, 28.8, 27.8	**0.95**, 0.93, 0.93
Overcast-sky LW↓						
Global	6871	316.2, 318.1, 316.4	**1.9**, 3.8, 2.0	**0.5**, 3.9, 2.8	**22.7**, 30.2, 30.2	**0.95**, 0.92, 0.92
Coastal	1502	362.0, 362.3, 360.5	3.2, 3.4, **1.7**	**2.7**, 5.6, 5.0	**14.7**, 29.6, 29.4	**0.97**, 0.88, 0.88
Desert	80	372.8, 387.2, 384.2	**0.1**, 14.4, 11.5	**0.9**, 16.8, 17.7	**18.6**, 40.3, 30.0	**0.94**, 0.74, 0.85
Island	275	425.4, 433.1, 433.2	**4.0**, 11.8, 11.8	**4.9**, 12.2, 11.9	**13.9**, 21.5, 22.5	**0.77**, 0.68, 0.64
Continental	2114	342.0, 344.4, 339.8	5.5, 7.9, **3.3**	**3.4**, 8.9, 5.7	**24.5**, 30.0, 32.0	**0.89**, 0.84, 0.81
Polar	2900	261.8, 263.3, 263.4	−1.6, −0.1, **0.0**	−5.1, −3.3, −**2.7**	**25.4**, 31.1, 29.9	**0.92**, 0.87, 0.88
Clear-sky LW↓						
Global	3794	248.9, 246.1, 244.3	−**8.9**, −11.6, −13.5	−**7.5**, −10.7, −11.4	**23.0**, 31.1, 31.4	**0.98**, 0.96, 0.96
Coastal	454	315.5, 302.7, 299.2	**1.4**, −11.4, −14.9	**1.0**, −8.9, −10.4	**11.9**, 40.6, 41.0	**0.98**, 0.77, 0.77
Desert	669	322.2, 326.9, 325.8	−21.6, −**16.8**, −18.0	−18.3, −12.4, −**9.8**	**31.1**, 35.1, 32.8	**0.86**, 0.74, 0.79
Island	48	385.8, 380.5, 380.5	**0.6**, −4.7, −4.7	−**1.5**, −6.9, −7.0	**9.2**, 12.8, 14.5	**0.92**, 0.90, 0.88
Continental	1233	303.9, 295.9, 293.0	−**4.3**, −12.3, −15.2	−**2.4**, −7.3, −9.5	**20.6**, 28.6, 31.7	**0.94**, 0.91, 0.89
Polar	1390	138.2, 140.0, 139.2	−10.6, −**8.8**, −9.6	−16.4, −**14.0**, −14.2	**23.6**, 27.8, 27.0	**0.93**, 0.88, 0.90

Table 3-3: Same as Table 3-1 but for nighttime LW surface downward flux.

	N	Mean flux	Bias ($\overline{\Delta}$)	Median Δ	RMSΔ	Correlation (*r*)
All-sky LW↓						
Global	15 568	267.9, 269.9, 271.2	−5.0, −3.0, −**1.6**	−7.9, −5.4, −**4.8**	**27.0**, 29.8, 30.3	**0.96**, 0.95, 0.95
Coastal	2895	332.4, 332.9, 331.9	−3.8, −**3.2**, −4.3	−6.2, −5.7, −**5.5**	**25.6**, 29.9, 27.7	**0.91**, 0.88, 0.90
Desert	928	310.4, 315.8, 316.5	−10.2, −4.8, −**4.1**	−8.4, −7.6, −**6.8**	**21.4**, 28.2, 25.1	**0.91**, 0.84, 0.88
Island	727	404.3, 407.4, 407.3	**1.9**, 5.1, 5.0	**2.6**, 4.3, 4.6	**16.1**, 20.4, 21.1	**0.83**, 0.76, 0.75
Continental	5269	295.4, 296.8, 299.0	−11.7, −10.3, −**8.1**	−10.3, −10.3, −**9.6**	**25.9**, 30.0, 30.8	**0.92**, 0.88, 0.87
Polar	5749	185.3, 187.7, 189.9	**0.6**, 3.0, 5.2	−7.1, −0.5, −**0.4**	**30.5**, 30.8, 32.6	**0.90**, 0.89, 0.89
Overcast-sky LW↓						
Global	7040	268.4, 270.6, 272.0	−6.1, −3.9, −**2.4**	−8.6, −5.8, −**4.9**	**27.2**, 29.9, 30.2	**0.96**, 0.95, 0.95
Coastal	1473	343.0, 348.6, 348.0	−8.1, −**2.4**, −3.1	−9.8, −5.0, −**4.5**	**26.6**, 32.6, 31.0	**0.90**, 0.84, 0.86
Desert	126	348.2, 362.0, 365.1	−12.9, **1.0**, 4.0	−15.1, −3.7, **0.3**	**22.9**, 29.0, 26.4	**0.91**, 0.83, 0.86
Island	311	415.0, 421.3, 422.3	**1.2**, 7.5, 8.6	**2.1**, 6.6, 7.8	**13.5**, 18.7, 19.3	**0.82**, 0.73, 0.74
Continental	2027	315.0, 320.9, 323.6	−15.6, −8.8, −**6.1**	−15.6, −11.0, −**10.0**	**31.9**, 34.1, 36.3	**0.84**, 0.78, 0.75
Polar	2588	224.0, 226.7, 229.0	−4.7, −2.1, **0.3**	−8.0, −5.4, −**3.2**	**29.6**, 32.2, 33.3	**0.81**, 0.77, 0.75
Clear-sky LW↓						
Global	3963	271.4, 273.4, 275.1	−4.7, −2.8, −**1.1**	−7.5, −5.3, −**4.7**	**26.3**, 29.4, 30.2	**0.96**, 0.95, 0.94
Coastal	574	302.8, 298.5, 296.9	−**1.1**, −5.3, −6.9	−**5.4**, −9.2, −9.2	**22.3**, 34.2, 33.7	**0.92**, 0.83, 0.84
Desert	566	297.6, 302.5, 303.5	−12.9, −8.0, −**7.0**	−10.4, −12.3, −**10.0**	**22.0**, 30.1, 27.1	**0.88**, 0.78, 0.83
Island	86	392.8, 389.4, 387.2	1.8, −**1.6**, −3.7	3.3, −**0.1**, 0.3	**15.9**, 18.4, 19.6	**0.78**, 0.72, 0.69
Continental	1580	274.3, 273.11, 276.1	−8.8, −10.0, −**7.0**	−**7.5**, −10.5, −9.5	**17.9**, 27.6, 29.3	**0.96**, 0.90, 0.88
Polar	1401	85.2, 96.1, 94.3	−14.6, −**3.7**, −5.5	−17.0, −**2.7**, −5.0	22.2, **19.3**, 21.9	**0.92**, 0.80, 0.75

4.0 References

Collins, W. D., P. J. Rasch, B. E. Eaton, B. V. Khattatov, J.-F. Lamarque, and C. S. Zender, 2001: Simulating aerosols using a chemical transport model with assimilation of satellite aerosol retrievals: Methodology for INDOEX. Journal of Geophysical Research: Atmospheres, 106 (D7), 7313–7336.

Fillmore, D. W., D. A. Rutan, S. Kato, F. G. Rose, and T. E. Caldwell, 2022: Evaluation of aerosol optical depths and clear-sky radiative fluxes of the CERES Edition 4.1 SYN1deg data product, Atmos. Chem. Phys., 22, 10115-10137.

Gupta, S. K., 1989: A parameterization for longwave surface radiation from sun-synchronous satellite data. J. Climate, 2, 305–320, https://doi.org/10.1175/1520-0442(1989)002<0305:APFLSR>2.0.CO;2.

Gupta, S. K., W. L. Darnell, and A. C. Wilber, 1992: A parameterization for longwave surface radiation from satellite data: Recent improvements. J. Appl. Meteor. Climatol., 31, 1361–1367, https://doi.org/10.1175/1520-0450(1992)031<1361:APFLSR>2.0.CO;2.

Gupta, S. K., D. P. Kratz, P. W. Stackhouse Jr., and A. C. Wilber, 2001: The Langley Parameterized Shortwave Algorithm (LPSA) for surface radiation budget studies. NASA Tech. Memo. NASA/TP-2001-211272, 31 pp.

Gupta, S. K., D. P. Kratz, P. W. Stackhouse Jr., A. C. Wilber, T. Zhang, and V. E. Sothcott, 2010: Improvement of surface longwave flux algorithms used in CERES processing. J. Appl. Meteor. Climatol., 49, 1579–1589, https://doi.org/10.1175/2010JAMC2463.1.

Ham, S.-H., S. Kato, and F. G. Rose, 2019: Impacts of partly cloudy pixels on shortwave broadband irradiance computations. J. Atmos. Oceanic Technol., 36, 369–386, https://doi.org/ 10.1175/JTECH-D-18-0153.1.

Ham, S.-H., S. Kato, and F. G. Rose, S. Sun-Mack, Y. Chen, W. F. Miller, and R. C. Scott, 2022: Combining cloud properties from CALIPSO, CloudSat, and MODIS for top-of-atmosphere shortwave broadband irradiance computations: Impact of cloud vertical profiles. J. Appl. Meteor. Climatol., 61, 1449–1471, https://doi.org/10.1175/JAMC-D-21-0260.1.

Ignatov, A., and Coauthors, 2005: Two MODIS aerosol products over ocean on the Terra and Aqua CERES SSF datasets. Journal of the Atmospheric Sciences, 62 (4), 1008–1031.

Jin, Z., T. P. Charlock, W. L. Smith Jr., and K. Rutledge, 2004: A parameterization of ocean surface albedo. Geophys. Res. Lett., 31, L22301, https://doi.org/10.1029/2004GL021180.

Kratz, D. P., P. W. Stackhouse Jr., S. K. Gupta, A. C. Wilber, P. Sawaengphokhai, and G. R. McGarragh, 2014: The Fast Longwave and Shortwave Flux (FLASHFlux) data product: Single-scanner footprint fluxes. J. Appl. Meteor. Climatol., 53, 1059–1079, https://doi.org/10.1175/JAMC-D-13-061.1.

Levy, R., S. Mattoo, L. Munchak, L. Remer, A. Sayer, F. Patadia, and N. Hsu, 2013: The Collection 6 MODIS aerosol products over land and ocean. Atmospheric Measurement Techniques, 6 (11), 2989–3034.

Minnis, P., and Coauthors, 2021: CERES MODIS cloud product retrievals for edition 4—Part I: Algorithm changes. IEEE Transactions on Geoscience and Remote Sensing, 59 (4), 2744–

2780.

Radkevich, A., K. Khlopenkov, D. Rutan, S. Kato, 2013: A Supplementary Clear-Sky Snow and Ice Recognition Technique for CERES Level 2 Products. J. Atmos. Oceanic Technol., 30(3), 557-568. doi: 10.1175/JTECH-D-12-00100.1.

Remer, L. A., and Coauthors, 2005: The MODIS aerosol algorithm, products, and validation. Journal of atmospheric sciences, 62 (4), 947–973.

Rose, F. G., D. A. Rutan, T. Charlock, G. L. Smith, and S. Kato, 2013: An algorithm for the constraining of radiative transfer calculations to CERES-observed broadband top-of-atmosphere irradiance. J. Atmos. Oceanic Technol., 30, 1091–1106, https://doi.org/10.1175/JTECH-D-12-00058.1.

Rutan, D., T. P. Charlock, F. Rose, S. Kato, S. Zentz, and L. Coleman, 2006: Global surface albedo from CERES/TERRA surface and atmospheric radiation budget (SARB) data product, Am. Meteorol. Soc., Boston, Mass.

Rutan, D., F. Rose, M. Roman, N. Manalo-Smith, C. Schaaf, and T. Charlock, 2009: Development and assessment of broadband surface albedo from Clouds and the Earth's Radiant Energy System Clouds and Radiation Swath data product. J. Geophys. Res., 114, D08125, https://doi.org/10.1029/2008JD010669.

Strahler, A. H., J. P. Muller, MODIS Science Team members, 1999: Algorithm Theoretical Basis Document Version 5.0, April 1999, available at https://modis.gsfc.nasa.gov/data/atbd/atbd_mod09.pdf

Scott, R. C., F. G. Rose, P. W. Stackhouse Jr., N. G. Loeb, S. Kato, D. R. Doelling, D. A. Rutan, P. C. Taylor, and W. L. Smith, Jr., 2022: Clouds and Earth's Radiant Energy System (CERES) Cloud Radiation Swath (CRS) Edition 4 Data product, J. Atmos. Oce. Tech., 39(11), 1781–1797, https://doi.org/10.1175/JTECH-D-22-0021.1

Yost, C. R., P. Minnis, S. Sun-Mack, Y. Chen, and W. L. Smith, 2020: CERES MODIS cloud product retrievals for Edition4 - Part II: Comparisons to CloudSat and CALIPSO. IEEE Trans. Geosci. Remote Sens., 59, 3695–3724, https://doi.org/10.1109/TGRS.2020.3015155.

5.0 Expected Reprocessing

In the longer term, advanced versions of CRS are expected. We anticipate uncertainties in the current version of the CRS product for

- SW and LW fluxes for mixed-phase clouds,
- SW fluxes over deep convective cloud regions due to large uncertainties in describing ice particle sizes from passive sensors,
- SW and LW fluxes for broken (partly) cloud regions,
- LW fluxes for multi-layered clouds, and
- Nighttime LW fluxes over polar regions due to the larger uncertainties in cloud detections and retrievals.

6.0 Attribution

When referring to the CERES CRS product, please include the product and data set version as "CERES Terra CRS Ed4A" or "CERES Aqua CRS Ed4A."

The CERES Team has gone to considerable trouble to remove major errors and to verify the quality and accuracy of this data. Please provide a reference to the following papers when you publish scientific results with the CERES Terra or Aqua Edition4 CRS data:

Wielicki, B. A., B. R. Barkstrom, E. F. Harrison, R. B. Lee III, G. L. Smith, and J. E. Cooper, 1996: Clouds and the Earth's Radiant Energy System (CERES): An Earth Observing System Experiment, Bull. Amer. Meteor. Soc., 77, 853-868.

Scott, R. C., F. G. Rose, P. W. Stackhouse Jr., N. G. Loeb, S. Kato, D. R. Doelling, D. A. Rutan, P. C. Taylor, and W. L. Smith, Jr., 2022: Clouds and Earth's Radiant Energy System (CERES) Cloud Radiation Swath (CRS) Edition 4 Data product, J. Atmos. Oce. Tech., 39(11), 1781–1797, https://doi.org/10.1175/JTECH-D-22-0021.1.

The CERES data products now have dois. To cite the data in publications use this format:

CERES Science Team, Hampton, VA, USA: NASA Atmospheric Science Data Center (ASDC), Accessed <**author citing data inserts date here**> at doi: (appropriate product)
10.5067/AQUA/CERES/CRS_AQUA-FM3_L2.004A
10.5067/TERRA/CERES/CRS_TERRA-FM1_L2.004A

When data from the Langley Data Center are used in a publication, we request the following acknowledgment be included: "These data were obtained from the Atmospheric Science Data Center at the NASA Langley Research Center."

The Langley Atmospheric Science Data Center requests two reprints of any published papers or reports or a brief description of other uses (e.g., posters, oral presentations, etc.) of data that we have distributed. This will help us determine the use of data that we distribute, which is important for optimizing product development. It also helps us to keep our product-related references current.

When CERES data obtained via the CERES web site are used in a publication, we request the following acknowledgment be included: "These data were obtained from the NASA Langley Research Center CERES ordering tool at https://ceres.larc.nasa.gov/data/."

7.0 Feedback

For questions or comments on the CERES CRS Data Quality Summary, contact the User and Data Services staff at the Atmospheric Science Data Center. For questions about the CERES subsetting/visualization/ordering tool at https://ceres.larc.nasa.gov/data/, please email LaRC-CERES-Help@mail.nasa.gov.

8.0 Document Revision Record

The Document Revision Record contains information pertaining to approved document changes. The table lists the Version Number, the date of the last revision, a short description of the revision, and the revised sections.

Document Revision Record

Version Number	Date	Description of Revision	Section(s) Affected
V1	05/03/2023	• New document.	All